

Enhanced precision of circadian rhythm by output system

Hotaka Kaji¹, Fumito Mori^{1, 2}, and Hiroshi Ito^{1, *}

¹Faculty of Design, Kyushu University, 4-9-1, Shiobaru, Fukuoka 815-8540, Japan

²Education and Research Center for Mathematical and Data Science, Kyushu University, Fukuoka 819-0395, Japan

*Correspondence: hito@design.kyushu-u.ac.jp

SUMMARY

Fluctuations in the oscillation period of cellular circadian rhythms are observed at a physiological level. The association between the fluctuation of the central circadian clock and its physiological output remains unknown. We developed a simple mathematical model representing a signal transduction from circadian clock to an output system and then numerically investigated the amount of fluctuation in the time interval between the peaks of the signals of clock and output. We found that the fluctuations in the output system were smaller than those in the circadian clock at an optimal degradation rate of the output molecules. In addition, analytical calculations validated the numerically-detected optimal degradation rate. Our theoretical findings suggest a design principle that the downstream can enhance the precision of the circadian rhythms.

INTRODUCTION

Circadian rhythms are physiological phenomena that repeat approximately every 24 hours. The one prominent property of circadian rhythm is self-sustainability,

that is, organisms can maintain their internal circadian oscillations under constant conditions (Johnson et al. [2004]). Recent single-cell observations have revealed that the individual cells show self-sustained circadian oscillation even if they are uncoupled, such as a dissociation culture. Moreover, the single-cellular rhythms show fluctuations, i.e., the period of circadian rhythm is irregular with a deviation (Micklem and Locke [2021]). Such fluctuation in rhythms can be quantified by coefficient of variation (CV), which is the standard deviation (SD) of the cycle-to-cycle periods divided by the average of those periods. For example, the oscillation period of mammalian fibroblast cell populations was 24.38 hours on average and fluctuated with SD of 1.12 hours (Li et al. [2020]), thus, $CV \sim 0.1$. The single-cell measurements for the *Arabidopsis* seedlings revealed $CV \sim 0.1$ (Gould et al. [2018]), which is close to mammalian cells. The circadian rhythm of prokaryote cyanobacteria is more accurate, with a period of 24.2 hours and SD of 0.12 hours, thus $CV \sim 0.005$ (Mihalcescu et al. [2004]).

The fluctuations in the circadian rhythms are partly because of fluctuations produced by the circadian molecular machinery (Chabot et al. [2007]). The circadian clock system of any organism involves a transcription-translation feedback loop (Nobel Prize Outreach AB). Thus, the feedback loop in the circadian clock system contains a transcriptional noise. This noise causes the dispersion of circadian period (Gonze et al. [2002]; Nishino et al. [2013]). In fact, the administration of a drug enhancing the transcriptional noise reduced the regularity of circadian oscillation (Li et al. [2020]).

The examples of precision of circadian rhythms described above were observed through the reporter system with bioluminescence or fluorescence. For example, Li et al. (Li et al. [2020]) used the reporter system that the clock-controlled Per2 promoter drives the expression of luciferase gene, resulting in daily rhythms of bioluminescence. Technically, fluctuations observed via these reporter systems are fluctuations of the output system. Some theoretical studies state that the signal transduction can amplify fluctuations (Shibata [2004], Shibata and Fujimoto [2005]). However, the association of fluctuations between the central circadian clock generating the circadian rhythms and the output system has been not addressed till date, because directly observing fluctuations of the central clock is difficult. Instead of experimental elucidation, we here theoretically addressed the question of whether

the precision of circadian clock is improved or worsened by the downstream of the clock.

Several studies on the fluctuation in the oscillation periods have ever been performed theoretically. The CV in the period of synchronized coupled phase oscillators was analytically and numerically analyzed (Kori et al. [2012], Mori and Kori [2013]). Conversely, the coupling strength can be inferred based on the deviation of the period (Mori and Kori [2022]). Moreover, Mori & Mikhailov derived a formula describing period variability in general N -dimensional oscillatory systems. The authors revealed that the accuracy of rhythm depends on the choice of output variables, suggesting that the fluctuation in clock and output can be different (Mori and Mikhailov [2016]).

This study considers a simple mathematical model consisting of a fluctuating circadian clock and its output system so that they are analytically tractable. By calculating the fluctuations of the circadian clock and the output system, we suggest a design principle for the precise biological rhythm.

RESULTS

Model

To investigate the transmission of fluctuation from a circadian clock to a reporter system (Figure 1A), we consider a coupled system consisting of the noisy phase oscillator and an output depending on the oscillator described by

$$\begin{aligned}\dot{\theta} &= \omega + \sqrt{D}\xi(t), \\ \dot{x} &= a + b \sin \theta(t) - Kx(t),\end{aligned}\tag{Equation 1}$$

where $\theta(t)$ is the phase of the circadian clock modulo 2π ; ω is the frequency; \sqrt{D} is the strength of noise, $\xi(t)$ is white Gaussian noise with $E[\xi(t)] = 0$ and $E[\xi(t)\xi(t')] = \delta(t - t')$, where E represents the expectation; x is the amount of reporter protein; a is a basal production rate; b is the coupling strength, and K is the degradation rate of the reporter protein. We assumed the clock-dependent production rate was represented as a sinusoidal function.

Numerical simulation showed the precision of output system depends on the degradation rate of reporter protein

We numerically solved Equation (1) and measured the variation of the oscillation periods of the central clock and output system. For a period of one cycle, we adopted peak-to-peak time interval of $\sin \theta$ and x , according to conventional chronobiology method (Figure 1A and Methods). Then, based on the measured mean and SD of the oscillation periods, we obtained CV as an index of the accuracy of rhythmicity.

The numerical simulation revealed that the degradation rate of reporter protein, K , modified the precision of the output rhythm (Figure 1B). For any value of K , the fluctuation of the output system was less than or equal to one of the central circadian clock. Moreover, $K \sim 10$ was an optimal value that minimizes the fluctuation in output periods. Interestingly, the CV was independent of the parameters involved in the protein synthesis, a and b , which will be confirmed by analytical calculation below.

Analytical calculation confirmed the numerical results

To understand the mechanism of precision enhancement of circadian oscillation, we performed analytical calculations. Mori and Mikhailov [2016] analytically calculated the oscillation precision for the general N -dimensional model,

$$\frac{d\mathbf{x}}{dt} = \mathbf{f}[\mathbf{x}(t)] + \epsilon \mathbf{G}[\mathbf{x}(t)] \boldsymbol{\xi}(t), \quad (\text{Equation 2})$$

where $\mathbf{x}(t)$ is a vector with N elements; \mathbf{f} represents the N -dimensional oscillatory system that generates a limit-cycle solution with period $\tau = 2\pi/\omega$ under noise-less conditions; $\epsilon \ll 1$ is the noise intensity; $\mathbf{G}[\mathbf{x}(t)]$ is a $N \times N$ diagonal matrix; and $\boldsymbol{\xi}(t)$ represents a vector of additive noise which holds $E[\xi_i] = 0$ and $E[\xi_i(t_1)\xi_j(t_2)] = \delta_{ij}\delta(t_1 - t_2)$. The authors derived the fluctuation in oscillation periods defined by intervals between checkpoints (See the legend for Figure 2A), which are expressed by three components as follows:

$$\text{CV} = \frac{\epsilon}{\tau} \sqrt{R_{\theta\theta} + R_{AA} + 2R_{\theta A}} + \mathcal{O}(\epsilon^2), \quad (\text{Equation 3})$$

where $R_{\theta\theta}$ is collective-phase diffusion, R_{AA} is the auto-correlation of amplitude deviation, and then $R_{\theta A}$ is cross correlation between the collective-phase shift and amplitude deviation. It had also been clarified that the CV depends on the choice of the observed variable and the checkpoint for observing periods as R_{AA} and $R_{\theta A}$ are dependent on them.

Equation (1) is a specific case of this general model, i.e., we can obtain Equation (1) by setting $\mathbf{f}[\mathbf{x}(t)] = \begin{bmatrix} \omega \\ a + b \sin \theta - Kx \end{bmatrix}$, $\epsilon = \sqrt{D}$, $\mathbf{G}[\mathbf{x}(t)] = \begin{bmatrix} 1 & 0 \\ 0 & 0 \end{bmatrix}$, and $\xi(t) = \begin{bmatrix} \xi(t) \\ 0 \end{bmatrix}$ in Equation (2). Therefore, Equation (3) is applicable to the present model, and provides CV values for both the clock and output systems.

First, we calculated the fluctuation in the period of circadian central clock. The three components in Equation (3) are

$$R_{\theta\theta} = \frac{\tau^2}{2\pi\omega}, \quad R_{AA} = 0, \quad R_{\theta A} = 0. \quad (\text{Equation 4})$$

The detailed derivation is presented in Methods section. As the clock does not have amplitude component, both R_{AA} and $R_{\theta A}$ for the clock are equal to 0. Consequently, the CV of the circadian clock is given by,

$$\text{CV}_{\text{clock}} = \sqrt{\frac{D}{2\pi\omega}}. \quad (\text{Equation 5})$$

It is understandable that CV_{clock} is a monotonically decreasing function of ω because more frequent oscillator receives less noise during one cycle.

Next, we calculated the CV of the oscillation periods of the output system. The three components in Equation (3) are

$$\begin{aligned} R_{\theta\theta} &= \frac{\tau^2}{2\pi\omega}, \\ R_{AA} &= \frac{\tau^2(1 - e^{-\kappa})}{2\pi\omega\kappa(\kappa^2 + 4\pi^2)} \cdot (\kappa^2 + 2\pi\kappa \tan \Phi_{\text{cp}} + 2\pi^2 + 2\pi^2 \tan^2 \Phi_{\text{cp}}), \\ R_{\theta A} &= -\frac{\tau^2(1 - e^{-\kappa})}{2\pi\omega\kappa(\kappa^2 + 4\pi^2)} \cdot (\kappa^2 + 2\pi\kappa \tan \Phi_{\text{cp}}), \end{aligned} \quad (\text{Equation 6})$$

where κ is the scaled degradation rate defined as $\kappa \equiv 2\pi K/\omega$. Φ_{cp} is the checkpoint

for observing periods (See Methods). Thus, we obtain

$$CV_{\text{output}} = \sqrt{\frac{D}{2\pi\omega}} \left[1 + \frac{1 - e^{-\kappa}}{\kappa(\kappa^2 + 4\pi^2)} (-\kappa^2 - 2\pi\kappa \tan \Phi_{\text{cp}} + 2\pi^2 + 2\pi^2 \tan^2 \Phi_{\text{cp}}) \right]. \quad (\text{Equation 7})$$

As in the numerical simulations, analytically calculated CV_{output} depends on the degradation rate κ , but not a and b . ω determines the scale of CV_{output} .

We visually compared the K -dependence of analytical and numerical CV under the fixed clock frequency, $\omega = 2\pi$ (rad/day). Both Equation (5) for CV_{clock} and Equation (7) for CV_{output} successfully reproduced the numerical results (Figure 2A). The CV_{output} has a minimum value around $K^* \sim 10$ (1/day), i.e., $\kappa^* = 2\pi \frac{K^*}{\omega} \sim 10$. This fact implies that the precision of the circadian rhythms can be enhanced in the downstream if the values of the frequency and decay rate are at the same order. When $K \rightarrow \infty$, the value of CV_{output} approaches the value of CV_{clock} , meaning that noise in the clock completely transmits to the downstream under the condition of frequent turnover of output protein. When $K \rightarrow 0$, CV_{output} converges to $\sqrt{\frac{D}{4\pi\omega}} (3 + \tan^2 \Phi_{\text{cp}})$. Such behaviors hold qualitatively regardless of the choice of checkpoint Φ_{cp} although CV_{output} depends on Φ_{cp} as in Equation (7).

We also visually checked the ω -dependence of CV (Figure 2B). As noted above, ω controls the absolute values of fluctuation rather than function form of CV. For the larger value of ω , the circadian clock and its output showed smaller fluctuations. This result is consistent with the observation that cultured mammalian cells with longer circadian period show less precise rhythm (Li et al. [2020], Nikhil et al. [2020]).

To examine the reason of enhanced precision in the downstream of clock, we visually decomposed CV_{output} into $R_{\theta\theta}$, R_{AA} and $R_{\theta A}$ for fixed ω (Figure 2C). $R_{\theta\theta}$ is positive and independent of K because this term comes from the fluctuation of the central clock. R_{AA} is also positive and monotonically decreasing function of K . $R_{\theta A}$ is always negative and a bowl-shaped function that has the minimum value around $K = 10$. Thus, the negative correlation of phase shift and amplitude variation contribute to the reduction of output fluctuation. Moreover, it seems that the fluctuation numerically measured by peak-to-peak cycle is coincident with $R_{\theta\theta} + 2R_{\theta A}$. This agreement suggests that peak-to-peak period is a more precise measure than

period measured via a checkpoint because of independence of amplitude deviation, R_{AA} .

DISCUSSION

We showed numerically and analytically that the clock and output of the circadian system differ in the amount of fluctuation of the oscillation period. Moreover, the peak-to-peak period of the output was more precise than that of the clock regardless of the parameters. The optimized degradation rate of the reporter protein improved precision of the output system. These results indicate that the output system not only transmits the time information to the physiological level, but also can embed the function of controlling the amount of fluctuation, which provides the new view of output system in circadian molecular machinery.

Among the parameters in the output system, only K was involved in the amount of fluctuations. This theoretical finding suggests that protein degradation controls the precision of the rhythm rather than protein synthesis. Moreover, we showed the optimal degradation rate was $K^* \sim 10$ (1/day), which corresponds to two hours in a half-life. In fact, the half-life of proteins in a living human cell ranges from 45 min to 22.5 hours (Eden et al. [2011]), suggesting that some proteins can contribute to the enhancement of precision in human circadian rhythm. In general, the downstream of the circadian clock consists of a complex metabolic network. Such a multi-step output pathway may be designed to further reduce fluctuations.

So far, Equation (1) was treated as the model describing circadian rhythms. However, other oscillatory phenomena in organisms, such as rhythmic firing of neurons and compression of cardiomyocytes, would require precise oscillations for proper biological functions. Therefore, the mechanism of output systems that make rhythms more precise could be discovered in existing biological oscillators other than circadian rhythms. Moreover, the concept of output-enhanced precision can be applied for synthetic oscillatory genetic circuits (Purcell et al. [2010]). It would be possible by controlling an output system to make a more accurate synthesized biological clock. Thus, this study provides a design principle for accurate oscillating circuits.

Limitations of the study

This study was performed from a theoretical point of view. Our conclusion that the output system can contribute to the precision of rhythmic period will need experimental validations. Since GFP variants with different stability had been developed (Andersen et al. [1998]), we can alter the value of degradation rate, K , by choosing different fluorescent genes in actual experiments. In addition, dilution due to cell division can also be an alternative parameter of K because it is involved in turn over of a fluorescent protein in a cell and can effectively control the degradation rate. Nutritional or thermal conditions also might control the precision of circadian rhythms through alteration of cell division rate.

Moreover, we can generalize our model because an analytically tractable model was employed. We have used a phase oscillator model for the circadian clock, which might be oversimplified. We assumed the synthetic rate for the reporter protein was represented as $a + b \sin \theta$. More generalized periodic function should be considered to confirm that our conclusions are not dependent on the assumptions.

ACKNOWLEDGMENTS

We thank I. Mihalcescu (Universite Grenoble Alpes) for a fruitful discussion. This work was supported in part by Japan Society for the Promotion of Science KAKENHI Grants JP18H05474 (H.I.), JP19K03663 (F. M.) and JP22K03453 (F. M.).

AUTHOR CONTRIBUTIONS

F. M. and H. I. conceived the project. H. K., F. M. and H. I. constructed the model and performed analytical calculation. H. K. performed the numerical simulation. H. K., F. M. and H. I. wrote the paper. All authors approved the final version of the manuscript.

DECLARATION OF INTERESTS

The authors declare no competing interests.

References

J. B. Andersen, C. Sternberg, L. K. Poulsen, S. P. Bjørn, M. Givskov, and S. Molin. New Unstable Variants of Green Fluorescent Protein for Studies of Transient Gene Expression in Bacteria. *Applied and Environmental Microbiology*, 64(6): 2240–2246, 1998. ISSN 0099-2240. doi: 10.1128/aem.64.6.2240-2246.1998.

J. R. Chabot, J. M. Pedraza, P. Luitel, and A. v. Oudenaarden. Stochastic gene expression out-of-steady-state in the cyanobacterial circadian clock. *Nature*, 450 (7173):1249, 12 2007. ISSN 1476-4687. doi: 10.1038/nature06395.

E. A. Coddington and R. Carlson. Linear ordinary differential equations, society for industrial and applied mathematics (siam), philadelphia, pa, 1997. *MR1450591*, *Zbl*, 1326.

E. Eden, N. Geva-Zatorsky, I. Issaeva, A. Cohen, E. Dekel, T. Danon, L. Cohen, A. Mayo, and U. Alon. Proteome Half-Life Dynamics in Living Human Cells. *Science*, 331(6018):764–768, 2011. ISSN 0036-8075. doi: 10.1126/science.1199784.

D. Gonze, J. Halloy, and A. Goldbeter. Robustness of circadian rhythms with respect to molecular noise. *Proceedings of the National Academy of Sciences*, 99 (2):673–678, 01 2002. ISSN 0027-8424. doi: 10.1073/pnas.022628299.

P. D. Gould, M. Domijan, M. Greenwood, I. T. Tokuda, H. Rees, L. Kozma-Bognar, A. J. Hall, and J. C. Locke. Coordination of robust single cell rhythms in the *Arabidopsis* circadian clock via spatial waves of gene expression. *eLife*, 7:e31700, 2018. doi: 10.7554/elife.31700.

C. Johnson, J. Elliott, R. Foster, K. Honma, and R. Kronauer. Fundamental properties of circadian rhythms. In J. Dunlap, J. Loros, and P. DeCoursey, editors, *Chronobiology: biological timekeeping*, chapter 3, pages 67–105. Sinauer Associates, Sunderland, MA, 2004.

H. Kori, Y. Kawamura, and N. Masuda. Structure of cell networks critically determines oscillation regularity. *Journal of Theoretical Biology*, 297:61–72, 2012. ISSN 0022-5193. doi: 10.1016/j.jtbi.2011.12.007.

Y. Li, Y. Shan, R. V. Desai, K. H. Cox, L. S. Weinberger, and J. S. Takahashi. Noise-driven cellular heterogeneity in circadian periodicity. *Proceedings of the National Academy of Sciences of the United States of America*, 117(19):10350–10356, 2020. ISSN 0027-8424. doi: 10.1073/pnas.1922388117.

C. N. Micklem and J. C. Locke. Cut the noise or couple up: Coordinating circadian and synthetic clocks. *iScience*, 24(9):103051, 2021. ISSN 2589-0042. doi: 10.1016/j.isci.2021.103051.

I. Mihalcescu, W. Hsing, and S. Leibler. Resilient circadian oscillator revealed in individual cyanobacteria. *Nature*, 430(6995):81, 07 2004. ISSN 1476-4687. doi: 10.1038/nature02533.

F. Mori and H. Kori. Period variability of coupled noisy oscillators. *Physical Review E*, 87(3):030901, 03 2013. ISSN 1539-3755. doi: 10.1103/physreve.87.030901.

F. Mori and H. Kori. Noninvasive inference methods for interaction and noise intensities of coupled oscillators using only spike time data. *Proceedings of the National Academy of Sciences*, 119(6):e2113620119, 2022. ISSN 0027-8424. doi: 10.1073/pnas.2113620119.

F. Mori and A. S. Mikhailov. Precision of collective oscillations in complex dynamical systems with noise. *Physical Review E*, 93(6):062206, 06 2016. ISSN 2470-0045. doi: 10.1103/physreve.93.062206.

K. L. Nikhil, S. Korge, and A. Kramer. Heritable gene expression variability and stochasticity govern clonal heterogeneity in circadian period. *PLoS Biology*, 18(8):e3000792, 2020. ISSN 1544-9173. doi: 10.1371/journal.pbio.3000792.

R. Nishino, T. Sakaue, and H. Nakanishi. Transcription Fluctuation Effects on Biochemical Oscillations. *PLoS ONE*, 8(4):e60938, 2013. doi: 10.1371/journal.pone.0060938.

Nobel Prize Outreach AB. Discoveries of molecular mechanisms controlling the circadian rhythm. <https://www.nobelprize.org/prizes/medicine/2017/advanced-information/>. Accessed: 31 May 2022.

O. Purcell, N. J. Savery, C. S. Grierson, and M. d. Bernardo. A comparative analysis of synthetic genetic oscillators. *Journal of The Royal Society Interface*, 7(52):1503–1524, 2010. ISSN 1742-5689. doi: 10.1098/rsif.2010.0183.

T. Shibata. Amplification of noise in a cascade chemical reaction. *Physical Review E*, 69(5):056218, 2004. ISSN 1539-3755. doi: 10.1103/physreve.69.056218.

T. Shibata and K. Fujimoto. Noisy signal amplification in ultrasensitive signal transduction. *Proceedings of the National Academy of Sciences of the United States of America*, 102(2):331–336, 2005. ISSN 0027-8424. doi: 10.1073/pnas.0403350102.

Figure Legends

Figure 1. Numerical observation of the fluctuation of the circadian clock and output system.

(A) Schematic diagram for the considered model. Circadian clock produces noisy circadian rhythms and periodically controls a promoter activity. The promoter fuses a reporter gene and then periodically drives its gene expression. To measure the fluctuation of the oscillation period in circadian clock and output system, we detected peaks of $\sin \theta$ and x , respectively. Then, we calculated the coefficient variations (CV) of time intervals between the peaks.

(B) Fluctuation of the oscillation periods in clock and output systems, based on numerical simulation for Equation (1), where $a = 1.0$, $b = 1.0$, $\omega = 2\pi$, and $D = 0.03$. CV of the oscillation period was measured for the different degradation constant K . The Error bars denote the standard error.

Figure 2. Analytical calculation for the fluctuation of the circadian clock and output system.

(A) Comparison of numerical and analytical calculations for the precision of cycles. We measured the oscillation period based on two different checkpoints, i.e., we defined the two thresholds at half ($\Phi_{cp} = 0$, left panel) and three-fourths ($\Phi_{cp} = \frac{\pi}{6}$, right panel) of the oscillatory range of $\sin \theta(t)$ or $x(t)$. We detected the times at which $\sin \theta(t)$ or $x(t)$ pass the thresholds from below to above. The period is defined as the interval of the detected times. The value of ω was fixed to 2π .

(B) Dependency of the precision of cycles on ω .
 (C) Dependency of $R_{\theta\theta}$, $2R_{\theta A}$, R_{AA} and $R_{\theta\theta} + 2R_{\theta A}$ on the degradation rate K .
 $\omega = 2\pi$, $\Phi_{cp} = 0\pi$. The square of CV_{output} in Figure 1B multiplied with $\left(\frac{\tau}{\sqrt{D}}\right)^2$ are plotted by yellow circles to compare with $R_{\theta\theta} + 2R_{\theta A}$.

METHODS

Analytical calculation for the precision of circadian rhythms

Based on the theory developed by Mori and Mikhailov [2016], we analytically derived the fluctuation in the oscillation period of the model Equation (1), which can be rewritten as

$$\frac{d\mathbf{x}}{dt} = \mathbf{f}[\mathbf{x}(t)] + \epsilon G[\mathbf{x}(t)]\boldsymbol{\xi}(t),$$

where $\mathbf{f}[\mathbf{x}(t)] = \begin{bmatrix} f_\theta(\theta, x) \\ f_x(\theta, x) \end{bmatrix} = \begin{bmatrix} \omega \\ a + b \sin \theta - Kx \end{bmatrix}$, $\epsilon = \sqrt{D}$, $\mathbf{G}[\mathbf{x}(t)] = \begin{bmatrix} 1 & 0 \\ 0 & 0 \end{bmatrix}$, and $\boldsymbol{\xi}(t) = \begin{bmatrix} \xi(t) \\ 0 \end{bmatrix}$. The solution for Equation (1) without noise ($D = 0$) is

$$\begin{aligned} \theta(t) &= \omega t + \theta(0) \bmod 2\pi, \\ x(t) &= \frac{a}{K} + \frac{b}{K^2 + \omega^2} [K \sin(\omega t + \theta(0)) - \omega \cos(\omega t + \theta(0))] \\ &\quad + \left[x(0) - \frac{a}{K} - \frac{b}{K^2 + \omega^2} (K \sin \theta(0) - \omega \cos \theta(0)) \right] e^{-Kt}. \end{aligned}$$

Thus, if the initial condition is set to $(\theta(0), x(0)) = \left(0, \frac{a}{K} - \frac{b\omega}{K^2 + \omega^2}\right)$, we get a limit cycle solution $\mathbf{p}(t)$ given by

$$\mathbf{p}(t) = \begin{bmatrix} \omega t \bmod 2\pi \\ \frac{a\tau}{\kappa} + \frac{b\tau}{\sqrt{\kappa^2 + 4\pi^2}} \sin(\omega t - \tan^{-1}(\frac{2\pi}{\kappa})) \end{bmatrix}, \quad (\text{Equation 8})$$

where $\kappa = 2\pi K / \omega$. Note that $\mathbf{p}(t)$ satisfies $\mathbf{p}(t) = \mathbf{p}(t + \tau)$, where the oscillation period without noise $\tau = 2\pi/\omega$.

Suppose that $\mathbf{x}(t)$ locates near the limit cycle, i.e., $\mathbf{x}(t)$ can be written as

$$\mathbf{x}(t) = \mathbf{p}(t) + \epsilon \mathbf{z}(t) + \mathcal{O}(\epsilon^2),$$

where $\|\mathbf{z}\| \ll \epsilon^{-1}$. Then, $\mathbf{z}(t)$ obeys the linearized equation

$$\frac{d\mathbf{z}}{dt} = \mathbf{\Gamma}(t)\mathbf{z}(t) + \mathbf{G}[\mathbf{p}(t)]\boldsymbol{\xi}(t),$$

where the Jacobian matrix $\mathbf{\Gamma}(t)$ is given by

$$\mathbf{\Gamma}(t) = \begin{bmatrix} \frac{\partial f_\theta}{\partial \theta} & \frac{\partial f_\theta}{\partial x} \\ \frac{\partial f_x}{\partial \theta} & \frac{\partial f_x}{\partial x} \end{bmatrix}_{\mathbf{x}(t)=\mathbf{p}(t)} = \begin{bmatrix} 0 & 0 \\ b \cos \omega t & -\frac{\kappa}{\tau} \end{bmatrix}.$$

Then, we considered the unperturbed system

$$\frac{d\mathbf{z}}{dt} = \mathbf{\Gamma}(t)\mathbf{z}(t) = \begin{bmatrix} 0 & 0 \\ b \cos \omega t & -\frac{\kappa}{\tau} \end{bmatrix} \begin{bmatrix} z_1(t) \\ z_2(t) \end{bmatrix}. \quad (\text{Equation 9})$$

Equation (9) can be solved with the initial value of $\mathbf{z}(0)$ as

$$\mathbf{z}(t) = \begin{bmatrix} 1 \\ \frac{b\tau}{\kappa^2+4\pi^2} \left\{ \sqrt{\kappa^2 + 4\pi^2} \cos(\omega t - \tan^{-1}(\frac{2\pi}{\kappa})) - \kappa e^{-\frac{\kappa}{\tau}t} \right\} \end{bmatrix} \begin{bmatrix} z_1(0) \\ z_2(0) \end{bmatrix}.$$

Moreover, we can rewrite $\mathbf{z}(t)$ as

$$\mathbf{z}(t) = \mathbf{U}(t)\mathbf{U}(0)^{-1}\mathbf{z}(0),$$

where $\mathbf{U}(t)$ is called a fundamental matrix solution, defined as

$$\mathbf{U}(t) = \begin{bmatrix} 1 & 0 \\ \frac{b\tau}{\kappa^2+4\pi^2} \left\{ \sqrt{\kappa^2 + 4\pi^2} \cos(\omega t - \tan^{-1}(\frac{2\pi}{\kappa})) - \kappa e^{-\frac{\kappa}{\tau}t} \right\} & e^{-\frac{\kappa}{\tau}t} \end{bmatrix}.$$

We introduce here the constant matrix \mathbf{B} and a periodic matrix function $\mathbf{P}(t)$, which are defined as

$$\begin{aligned} \exp(\tau\mathbf{B}) &\equiv \mathbf{U}(0)^{-1}\mathbf{U}(\tau), \\ \mathbf{P}(t) &\equiv \mathbf{U}(t)e^{-t\mathbf{B}}. \end{aligned}$$

For our model, \mathbf{B} and $\mathbf{P}(t)$ are

$$\mathbf{B} = \begin{bmatrix} 0 & 0 \\ \frac{b\kappa^2}{\kappa^2+4\pi^2} & -\frac{\kappa}{\tau} \end{bmatrix}$$

$$\mathbf{P}(t) = \begin{bmatrix} 1 & 0 \\ \frac{b\tau}{\kappa^2+4\pi^2} \left\{ \sqrt{\kappa^2 + 4\pi^2} \cos(\omega t - \tan^{-1}(\frac{2\pi}{\kappa})) - \kappa \right\} & 1 \end{bmatrix}.$$

Thus, we get the right and left eigenvector of \mathbf{B} , ϕ and ${}^t\psi$, respectively, where the superscript t implies the transposition. According to Floquet theory (Coddington and Carlson), the eigenvalues of \mathbf{B} are called Floquet exponents, and one of the Floquet components should be zero because we consider the model showing the limit cycle oscillations. In fact, the eigenvalues of \mathbf{B} are $\lambda_0 = 0$, and $\lambda_1 = -\kappa/\tau$.

For $\lambda_0 = 0$, we get

$$\phi_0 = \begin{bmatrix} \omega \\ \frac{2\pi b\kappa}{\kappa^2+4\pi^2} \end{bmatrix}, \quad \psi_0 = \begin{bmatrix} \frac{1}{\omega} \\ 0 \end{bmatrix}.$$

For $\lambda_1 = -\kappa/\tau$, we get

$$\phi_1 = \begin{bmatrix} 0 \\ 1 \end{bmatrix}, \quad \psi_1 = \begin{bmatrix} \frac{-b\tau\kappa}{\kappa^2+4\pi^2} \\ 1 \end{bmatrix}.$$

According to the Mori and Mikhailov [2016], we can calculate the CV of the oscillation periods based on the three components,

$$\text{CV} = \frac{\epsilon}{\tau} \sqrt{R_{\theta\theta} + R_{AA} + 2R_{\theta A}} + \mathcal{O}(\epsilon^2),$$

where $R_{\theta\theta}$, R_{AA} , and $R_{\theta A}$ correspond to collective-phase diffusion, the auto-correlation of amplitude deviation, and cross correlation between the collective-phase shift and the amplitude deviation, respectively. These components can be expressed with $\mathbf{P}(t)$, $\phi_{0,1}$, and $\psi_{0,1}$, as following,

$$\begin{aligned}
R_{\theta\theta} &= \int_0^\tau {}^t\psi_0 \mathbf{P}(t)^{-1} \mathbf{G}[\mathbf{p}(t)]^2 {}^t\mathbf{P}(t)^{-1} \psi_0 dt, \\
R_{AA} &= \sum_{j=1}^{N-1} \sum_{k=1}^{N-1} [2 - \exp(\lambda_j \tau) - \exp(\lambda_k \tau)] \frac{[\mathbf{P}(t_{\text{cp}})\phi_j]_l [\mathbf{P}(t_{\text{cp}})\phi_k]_l}{[\dot{\mathbf{p}}(t_{\text{cp}})]_l^2} \exp[(\lambda_j + \lambda_k)t_{\text{cp}}] \\
&\quad \times \left\{ \int_0^{t_{\text{cp}}} \exp[-(\lambda_j + \lambda_k)t] {}^t\psi_j \mathbf{P}(t)^{-1} \mathbf{G}[\mathbf{p}(t)]^2 {}^t\mathbf{P}(t)^{-1} \psi_k dt \right. \\
&\quad \left. + \frac{\exp[(\lambda_j + \lambda_k)\tau]}{1 - \exp[(\lambda_j + \lambda_k)\tau]} \int_0^\tau \exp[-(\lambda_j + \lambda_k)t] {}^t\psi_j \mathbf{P}(t)^{-1} \mathbf{G}[\mathbf{p}(t)]^2 {}^t\mathbf{P}(t)^{-1} \psi_j dt \right\}, \\
R_{\theta A} &= \sum_{j=1}^{N-1} \exp(\lambda_j \tau) \frac{[\mathbf{P}(t_{\text{cp}})\phi_j]_l}{[\dot{\mathbf{p}}(t_{\text{cp}})]_l} \\
&\quad \times \int_0^\tau \exp(-\lambda_j t) {}^t\psi_0 \mathbf{P}(t_{\text{cp}} + t)^{-1} \mathbf{G}[\mathbf{p}(t + t_{\text{cp}})]^2 {}^t\mathbf{P}(t_{\text{cp}} + t)^{-1} \psi_j dt,
\end{aligned} \tag{Equation 10}$$

where N is the dimension of the considered system, thus $N = 2$; $[\mathbf{x}]_l$ denotes the l th element of the vector \mathbf{x} ; $l = 1$ and $l = 2$ are substituted for CV_{clock} and $\text{CV}_{\text{output}}$, respectively; t_{cp} is the time determined based on choice of checkpoint, which is defined at the subsection of "Measurement of fluctuation in peak-to-peak periods".

Based on Equation (10), we obtain $R_{\theta\theta}$, R_{AA} , and $R_{\theta A}$ as shown in Equation (4) and Equation (6).

Numerical Simulation

Equation (1) was numerically solved for 1000 cycles with Euler's method where $\Delta t = 0.0001$. The initial value of $(\theta(0), x(0))$ was set to $(0, \frac{1}{K} - \frac{2\pi}{K^2 + 4\pi^2})$, which is on the limit cycle, Equation (8). We numerically obtained the CV in the simulation, and repeated it 10 times for averaging the CV values.

Measurement of fluctuation in peak-to-peak periods

For Figure 1B, we measured the fluctuations in peak-to-peak periods of the clock and the output. We detected the peaks of $\sin \theta(t)$ and $x(t)$ with the function in the module of Python3, `scipy.signal.argrelextrema`.

Measurement of fluctuation in periods determined by a checkpoint

For Figure 2A, we set two different checkpoints to measure the oscillation periods of $\sin \theta(t)$ and $x(t)$. The limit cycle for our model under noise-free conditions, Equation (8), can be rewritten as

$$\begin{aligned}\sin \theta(t) &= \sin \omega t, \\ x(t) &= \frac{a\tau}{\kappa} + \frac{b\tau}{\sqrt{\kappa^2 + 4\pi^2}} \sin \left(\omega t - \tan^{-1} \left(\frac{2\pi}{\kappa} \right) \right),\end{aligned}$$

or,

$$\begin{aligned}\sin \theta(t) &= \sin \Phi^{\text{clock}}(t), \\ x(t) &= \frac{a\tau}{\kappa} + \frac{b\tau}{\sqrt{\kappa^2 + 4\pi^2}} \sin \Phi^{\text{output}}(t),\end{aligned}$$

by introducing the apparent phase on the limit cycle, $\Phi^{\text{clock}}(t) \equiv \omega t$ and $\Phi^{\text{output}}(t) \equiv \omega t - \tan^{-1}(2\pi/\kappa)$. Note that $\Phi^{\text{output}}(t)$ is dependent on the values of ω and κ , i.e., $K (= \kappa\omega/2\pi)$.

Then, we employed the two checkpoints: $\Phi_{\text{cp}} = 0\pi$ and $\frac{\pi}{6}$. In other words, we provided the two thresholds, which are at the half and three-fourths of the oscillatory range of $\sin \Phi^{\text{clock}}(t)$ and $\sin \Phi^{\text{output}}(t)$.

For the numerical analysis, we recorded the times at which $\sin \theta(t)$ and $x(t)$ pass the thresholds, $\sin \Phi_{\text{cp}}$ and $\frac{a\tau}{\kappa} + \frac{b\tau}{\sqrt{\kappa^2 + 4\pi^2}} \sin \Phi_{\text{cp}}$, from below to above, respectively. Then, we calculated the value of CV based on the time intervals. For large noise cases, $x(t)$ may not exceed these thresholds. In our simulations, when $x(t)$ did not exceed the threshold during each cycle even once, we discarded the whole time series. The Python code for this procedure is provided through the website in github below: <https://github.com/hito1979/outputnoise>.

For analytical calculation of Equation (4) and Equation (6), we used Equation (10), which contains the parameter t_{cp} . $t_{\text{cp}}^{\text{clock}}$ and $t_{\text{cp}}^{\text{output}}$ were determined by common Φ_{cp} :

$$\begin{aligned}t_{\text{cp}}^{\text{clock}} &= \frac{\Phi_{\text{cp}}}{\omega}, \\ t_{\text{cp}}^{\text{output}} &= \frac{\tan^{-1}(\frac{2\pi}{\kappa}) + \Phi_{\text{cp}}}{\omega}.\end{aligned}$$

Figure 1

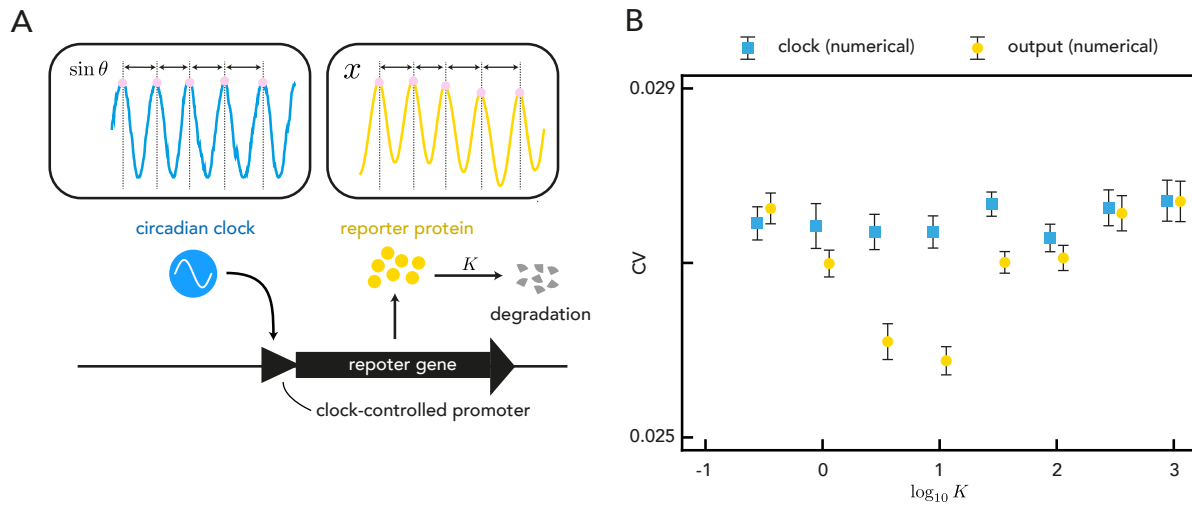


Figure 2

